


ORIGINAL ARTICLE

Dose Assessment in Radiotherapy of Head and Neck Cancer after Metal Artifact Reduction in Neusoft-Philips Corporation CT Scanner: A Clinical Study

Azam Abedini ¹, Kourosh Ebrahimnejad Gorji ², Naser Ghaemian ³, Sakineh Soleimani Varaki ^{4,5}, Mohammad Davoudi ⁶, Alaba Tolulope Agbele ^{7,8}, Ali Shabestani Monfared ^{9*} 

¹ Student Research Committee, Babol University of Medical Sciences, Babol, Iran

² Department of Medical Physics Radiobiology and Radiation Protection, School of Medicine, Babol University of Medical Sciences, Babol, Iran

³ Department of Pediatric Radiology, Babol University of Medical Sciences, Babol, Iran

⁴ Radiation Oncologist, Babol University of Medical Sciences, Babol, Iran

⁵ Department of Radiotherapy and Oncology, Shahid Rajaei Hospital, Babolsar, Iran

⁶ Department of Medical Imaging Center, Babol University of Medical Sciences, Babol, Iran

⁷ Department of Medical Physics, Tehran University of Medical Sciences, Tehran, Iran

⁸ Department of X-Ray, College of Health Sciences and Technology, Ijero Ekiti

⁹ Cancer Research Center, Health Research Institute, Babol University of Medical Sciences, Babol, Iran

*Corresponding Author: Ali Shabestani Monfared
Email: monfared1345@gmail.com

Received: 26 December 2021 / Accepted: 12 February 2022

Abstract

Purpose: Metal artifacts cause to increase in the uncorrected dose evaluation during radiotherapy planning. This study aimed to evaluate the probable difference of the dose parameters calculated by the Treatment Planning System (TPS) in radiotherapy of head and neck cancer before and after metal artifact correction in Neusoft-Philips Corporation Computed Tomography (CT) images.

Materials and Methods: In the present study, the radiotherapy planning of the head and neck cancer from thirty patients was first performed on the CT default images with dental implants. The same processes were applied after performing a body standard metal kernel on the CT images to reduce the metal artifacts. The Gross Tumor Volume (GTV) and Organ At Risks (OARs) were contoured on the CT slices. The dosimetric parameters (mean, minimum, and maximum) for the GTV and OARs (eyes and spinal cord) were obtained for both sets of CT images (defaults and filtered). Wilcoxon signed-rank test was used to calculate the probability dose variations between the two sets.

Results: There are significant differences in several dose parameters between the default and filtered CT images (P-value < 0.05). These dosimetric parameters are related to the GTV (mean dose), spinal cord (minimum and mean doses), right eye (maximum dose), as well as left eye (mean dose). The average range of dose differences between the default and filtered images was obtained; 1.12%-3.11% for the GTV as well as 0.22%-12.05% for the OARs.

Conclusion: Based on the results, the body standard metal kernel can cause a significant difference in several dosimetric parameters of GTV and OARs during the radiotherapy of head and neck cancer. Therefore, it is recommended to make a metal artifact correction on CT images for accurate dose calculation before designing a treatment plan.

Keywords: Computed Tomography; Radiotherapy; Metal Artifacts; Head and Neck Tumors; Dose.

1. Introduction

Computed Tomography (CT) is a medical imaging modality that is commonly used to diagnose diseases [1–4]. However, metal implants after surgery can cause imaging artifacts during CT scans, which invariably decrease the image quality [5–7].

Artifact problems are more considerable for patients during the treatment planning of radiation therapy. In radiotherapy, CT images are a common method used for designing the treatment planning process. Notably, treatment planning based on CT images serves two main purposes in radiotherapy; it defines the target areas and Organ At Risks (OARs) and provides the basis for calculating dose deposition in the target [6]. If the artifacts in CT images do not decrease, it will cause errors in CT numbers, consequently, dose calculation errors in radiation therapy [5,8].

Several commercial algorithms are used in reducing metal artifacts and their impact has been assessed in previous studies [5,7,9,10]. Most studies have assessed the image quality on the phantoms [11–13], and the dose values in radiotherapy after the use of commercial algorithms [11,14]. For instance, Huang *et al.* [5] investigated the effects of three artifacts' reduction methods, including a Metal Artifact Reduction algorithm for Orthopedic implants (O-MAR), monochromatic Gemstone Spectral Imaging (GSI), and GSI monochromatic along with metal artifact software using three anthropomorphic phantoms (hip prosthesis, dental fillings, and spinal fixation rods). In addition, Li *et al.* [11] reported that O-MAR could improve CT number accuracy, noise, as well as image quality in hip prostheses (in the phantom model) with the purpose of radiation therapy for prostate cancer.

Metallic fillings and dental implants often produce image artifacts during neck CT scans. These cause beam hardening, and photon starvation due to the high attenuation which could affect dose calculation during the radiation treatment procedures of the head and neck cancer [6]. In other words, metallic implants artifact in CT images around the head and neck regions may decrease or increase in the dose received due to their higher effective atomic number than the normal body tissues.

Since the issues mentioned above related to the metal artifacts could reduce the radiation treatment quality of head and neck cancer, appropriate methods should be

performed. Washio *et al.* [15] investigated the effects of the iterative Cone-Beam Computed Tomography (CBCT) reconstruction algorithm on the metal artifacts during the radiation therapy of head and neck cancer in phantoms and clinical patients. In another study, Hansen *et al.* [] assessed the impact of the O-MAR algorithm in CT images of head and neck regions. The accuracy and dose calculation precision of the Gross Tumor Volume (GTV) and OARs, were investigated after Metal Artifact Reduction (MAR) during radiotherapy.

To the best of our knowledge, there is no study using “body standard metal reconstruction”, in the Neusoft-Philips Corporation CT scanner to clarify its effectiveness on the dose parameters during radiotherapy of head and neck cancer. In the current study, the CT images of the neck regions were performed with and without the use of a body standard metal kernel (the application of dedicated reconstruction kernels). To do this, the planning process of head and neck cancer was applied using the Treatment Planning System (TPS) in radiotherapy for the two sets of images to assess the effect of the application on the dose parameters for GTV and OARs.

2. Materials and Methods

2.1. Patients and CT Imaging

A national ethics committee approved the study protocol and waived the informed consent requirement. Thirty patients were assessed retrospectively and randomly, aged 31 to 68 years (12 males and 18 females, with a mean age of 49.5 ± 14) with dental metal prostheses or implants undergoing radiotherapy of head and neck cancer.

The CT images from the patients were carried out using a dual CT scanner (Neusoft-Philips Corporation, neuViz dual MX8000, China). The CT parameters for the neck regions are depicted in Table 1. In addition, the CT scanner

Table 1. Scan and dose parameters for the neck region

Parameter	Value
Tube voltage (kVp)	120
Effective tube current-time product (mAs)	110
Collimation (mm)	2*2.5
Image slice thickness (mm)	2.5
Pitch	1.45
CTDI_w (mGy)	17.7 ± 1.5
CTDI_{vol} (mGy)	12.2 ± 1.5
DLP (mGy.cm)	238 ± 5

is calibrated periodically every 6 months. Furthermore, the patients were scanned in the supine position and all images were taken without any contrast-enhanced.

2.2. Radiotherapy and Treatment Planning Procedures

The patients were treated using a 6-MV photon beam from Primus accelerator (Siemens primus, USA) with TiGRT TPS (v. 1.2, LinaTech, Sunnyvale, CA, USA). The CT data were transferred to the TPS for contouring. A physician-contoured GTV and OARs on the CT slices. The right and left eyes, and the spinal cord were investigated as the OARs in the current study.

The prescribed dose for the treatment planning of radiation therapy of head and neck cancer was considered according to the guidelines from the Danish Head and Neck Cancer Group (DAHANCA), which was 46 Gy in 23 fractions, 2 Gy per session [16].

For each patient, two lateral fields were used for radiation therapy. The dose calculations were performed using an exclusive algorithm, known as Full Scatter Convolution (FSC) in TiGRT software. Dosimetry voxels sizes were chosen $3 \times 3 \times 3 \text{ mm}^3$, and calculated doses in the voxels belonging to each contoured organ were used to obtain minimum (minimum value among the voxels), maximum (maximum value among the voxels), as well as a mean dose of the organ.

2.3. Dose Differences between the Two Sets of the Images

The body standard metal reconstruction algorithm used in the current study is an iterative loop where the output correction image is subtracted from the primary input image, and the resultant image then becomes the new input image and the process can be repeated.

Two image sets were used for dose calculation; the images without MAR filter and the images obtained after applying MAR filter. Before and after the use of MAR filters, all image sets were visually reviewed by an experienced radiation oncologist and another

radiologist to validate whether the reconstruction filter was appropriate. The dose differences for each of the investigated dosimetric parameters were calculated using the following Equations 1, 2.

2.4. Statistical Analyses

Statistical analyses were performed using GraphPad Prism version 6 software. The Kolmogorov-Smirnov test was used to evaluate the distribution of continuous variables. Wilcoxon signed-rank test was used to evaluate the probability dose variations between defaults and filtered CT images. A P-value of less than 0.05 was considered statistically significant in all analyses.

3. Results

Figure 1 shows a sample of default and filtered neck CT images. The mean, minimum, and maximum dose values of the GTV and also for the investigated OARs (eyes and spinal cord) have been shown in the box plots (Figures 2, 3, and 4) in both default and filtered reconstruction methods.

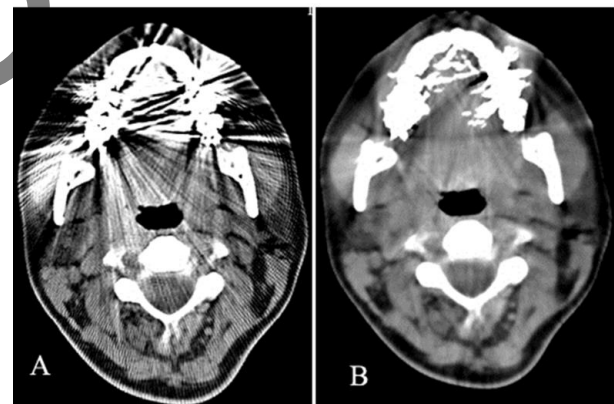


Figure 1. An example of neck CT images before (A) and after (B) performing the filter of “body standard metal kernel”

In the head and neck regions where targets and critical organs are located very close to dental restorations, any method that leads to artifacts’ reduction would have a greater impact on dose calculation. Several MAR options are available for CT imaging and their impact has been

$$\text{Dose difference}(\%) = \frac{\sum_{n=1}^{30} \left(\frac{\text{Dose (without MAR filter)} - \text{Dose (with MAR filter)}}{\text{Dose (without MAR filter)}} \right)}{n} * 100 \quad (1)$$

$$\text{Absolute dose difference}(\%) = \frac{\sum_{n=1}^{30} \left(\frac{|\text{Dose (without MAR filter)} - \text{Dose (with MAR filter)}|}{\text{Dose (without MAR filter)}} \right)}{n} * 100 \quad (2)$$

reported in previous studies [5–7,15,18,19]. However, according to our search, no investigations have been carried out on the “body standard metal filter”, installed on the Neusoft-Philips Corporation CT scanner, used as a MAR for the dental implants for treatment planning of head and neck cancers.

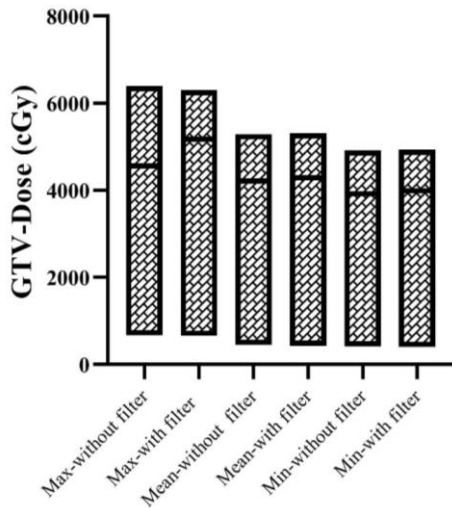


Figure 2. A box plot of the parameters (maximum, minimum, and mean values) related to the GTV, with and without using of “body standard metal kernel” during the radiotherapy planning of head and neck cancer

Table 2 presents the dosimetric parameter differences (percentage value and mathematical absolute percentage value) obtained from the CT images with and without using the MAR algorithm. According to this table, the dose differences were statistically significant (P-value < 0.05) for the GTV (mean dose), spinal cord (minimum and mean doses), right eye (maximum dose), as well as left eye (mean dose). The other dosimetric parameters had no significant differences (P-value > 0.05). Furthermore, the dose differences for the eyes were more remarkable.

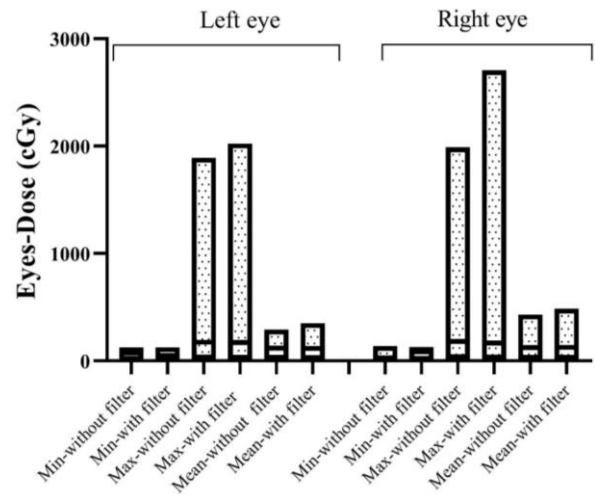


Figure 3. A box plot of the parameters (maximum, minimum, and mean values) related to the eyes, with and without using of “body standard metal kernel” during the radiotherapy planning of head and neck cancer

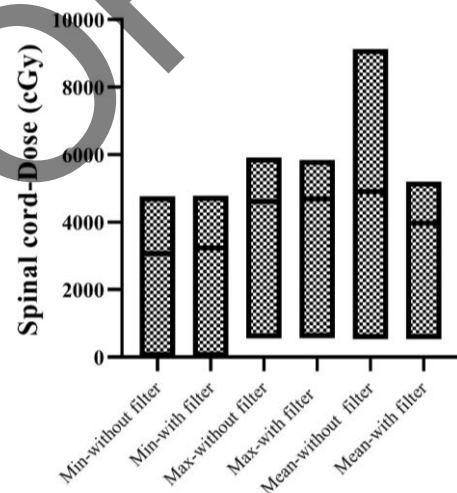


Figure 4. A box plot of the parameters (maximum, minimum, and mean values) related to the spinal cord, with and without using of “body standard metal kernel” during the radiotherapy planning of head and neck cancer

Table 2. Dose differences in the presence of “body standard metal kernel” on the parameters of the GTV and OARs

Parameters	GTV			Left eye			Right eye			Spinal cord		
	Max	Min	Mean	Max	Min	Mean	Max	Min	Mean	Max	Min	Mean
Average of dose differences (%)	-3.11	-1.75	-1.12	-7.24	-12.05	-10.07	-0.22	+6.13	-10.76	-0.95	+9.89	-8.02
Average of absolute dose differences (%)	8.20	4.13	1.50	19.51	25.27	19.41	25.10	91.36	18.51	2.12	11.42	7.93
P-value	0.315	0.263	0.001	0.051	0.060	0.038	0.038	0.674	0.089	0.569	0.001	0.003

Minus sign, “-”, means a decrease in the dose value in the presence of the filter (%).

Plus sign, “+”, means an increase in the dose value in the presence of the filter (%).

4. Discussion

In general, CT images are used to assign densities for heterogeneous dose calculations for radiation therapy treatment planning. However, beam hardening, photon starvation, scatter, edge effects, as well as patient motion results in CT imaging artifacts [9,17].

There are some other factors/ways which can help to reduce the dental metal artifact; modifying the scan parameters [20], the use of Magnetic Resonance Imaging (MRI) instead of CT modality [21], manual choice of Hounsfield Unit (HU) instead of the automated choice on the CT imaging during the treatment planning process, and avoiding metal implants during the CT scanning range [21].

Our clinical patient study showed that “body standard metal kernel” can reduce dental metal artifacts and remarkably improve soft tissue visualization during the radiotherapy of head and neck cancer. The results revealed that the average range of dose differences between the default and filtered images was obtained at 0.22-12.05% for the OAR and 1.12-3.11% for the GTV, but, in other related studies, different variations were obtained. For instance, in Hansen *et al.*'s [6] study, the dose difference was obtained at 22% for the GTV of 30 head and neck cancer patients when O-MAR algorithm was used. In their study, the dose difference for the parotid as OARs was obtained at 7% which is in line with the present study, however, the OARs were chosen for eyes and spinal cord in our study. In another study by Andersson *et al.* [22], they evaluated O-MAR (Philips) and iMAR (Siemens) CT algorithms in an anthropomorphic head phantom with dental fillings or neck implants. Their dosimetrically evaluation in proton treatment planning in the head and neck area has shown that MAR algorithms reduced the deviations in several dosimetric parameters, and improved the image quality

(for both target and OAR), with a better result of O-MAR. Discrepancies are related to the use of different types of CT scans and algorithms. In addition, various sizes and types of implants (titanium and steel) lead to different results.

5. Conclusion

According to the results of our clinical study, several dosimetric parameters in the radiotherapy of head and neck cancer differed significantly when the “body standard metal kernel” was used in the Neusoft-Philips Corporation CT scanner to reduce the metal artifacts. Therefore, the relevant kernel in the CT scanner can be used for images of head and neck regions for further treatment procedures.

Moreover, the type of TPS algorithms and operator experience are other main factors. Table 3 summarizes the dose differences between default and filtered reconstruction methods in some related studies performed on the phantom/patient compared with the present study.

There are some limitations in the present study. First of all, we have investigated the kernel only in a dual slice CT scan. Secondly, the quantity of noise was not assessed. Nevertheless, the effect of the size, the materials of the dental implants, as well as the location of dental implants were not investigated in the current research. Moreover, we only studied one scanning parameter; different tube voltages may result in a better artifact reduction. Thus, for future study, a more extensive evaluation on “body standard metal kernel” would be more desirable: as this can be implemented on other regions/organs considering the location, material, and size of implants or prostheses and combined with the other factors to reduce more dose variations in a multislice CT scanner.

Table 3. Dose differences between default and filtered reconstructions compared with several related studies

Study	Year	Study type	CT model	Algorithm/application	Dose differences (%)	
					GTV	OARs
Present study	2021	Patient	Neusoft-Philips Corporation	Body standard metal filter	1.12-3.11	0.22-12.05
Hansen <i>et al.</i> [6]	2017	Patient	Philips	O-MAR	22.00	7.00
Andersson <i>et al.</i> [22]	2018	Phantom	Philips and Siemens	O-MAR and iMAR	0.20-0.30	1.00
Sillanpaa <i>et al.</i> [10]	2020	Patient	Philips	O-MAR	4.20	0.77

Acknowledgments

This research was supported by Babol University of Medical Sciences (Babol, Iran). The authors would like to appreciate the manager and staff of Shahid Rajaei Hospital (Babolsar, Iran) for their sincere cooperation.

References

- 1- Davoudi M, Khoramian D, Abedi-Firouzjah R, Ataei G. "Strategy of computed tomography image optimisation in cervical vertebrae and neck soft tissue in emergency patients.", *Radiat Prot Dosimetry*.;187(1):98–102, (2019).
- 2- Khoramian D, Sistani S, Firouzjah RA. "Assessment and comparison of radiation dose and image quality in multi-detector CT scanners in non-contrast head and neck examinations.", *Pol J Radiol*. (2019); 84:e61.
- 3- Kiapour M, Gorji KE, Mehraeen R, Ghaemian N, Sustani FN, Abedi-Firouzjah R, *et al*. "Can Common Lead Apron in Testes Region Cause Radiation Dose Reduction during Chest CT Scan? A Patient Study.", *J Biomed Phys Eng*;11(4):497, (2021).
- 4- Awe OO, Obed RI, Adekanmi AJ, Ogbole GI, Agbele AT. "Thyroid dose and cancer risk from head and neck computed tomography at two selected centres in Nigeria.", *Niger Postgrad Med J*.;28(4):278, (2021).
- 5- Huang JY, Kerns JR, Nute JL, Liu X, Balter PA, Stingo FC, *et al*. "An evaluation of three commercially available metal artifact reduction methods for CT imaging." *Phys Med Biol*.;60(3):1047, (2015).
- 6- Hansen CR, Christiansen RL, Lorenzen EL, Bertelsen AS, Asmussen JT, Gyldenkerne N, *et al*. "Contouring and dose calculation in head and neck cancer radiotherapy after reduction of metal artifacts in CT images." *Acta Oncol*.;56(6):874–8, (2017).
- 7- Bazalova M, Beaulieu L, Palefsky S, Verhaegen F. "Correction of CT artifacts and its influence on Monte Carlo dose calculations.", *Med Phys*.;34(6Part1):2119–32, (2007).
- 8- Kilby W, Sage J, Rabett V. "Tolerance levels for quality assurance of electron density values generated from CT in radiotherapy treatment planning.", *Phys Med Biol*.;47(9):1485, (2002).
- 9- Boas FE, Fleischmann D. "Evaluation of two iterative techniques for reducing metal artifacts in computed tomography.", *Radiology*.;259(3):894–902, (2011).
- 10- Spadea MF, Verburg JM, Baroni G, Seco J. "The impact of low-Z and high-Z metal implants in IMRT: a Monte Carlo study of dose inaccuracies in commercial dose algorithms.", *Med Phys*.;41(1):011702, (2014).
- 11- Li H, Noel C, Chen H, Harold Li H, Low D, Moore K, *et al*. "Clinical evaluation of a commercial orthopedic metal artifact reduction tool for CT simulations in radiation therapy.", *Med Phys*.;39(12):7507–17, (2012).
- 12- Hilgers G, Nuver T, Minken A. "The CT number accuracy of a novel commercial metal artifact reduction algorithm for large orthopedic implants.", *J Appl Clin Med Phys*.;15(1):274–8, (2014).
- 13- Glide-Hurst C, Chen D, Zhong H, Chetty IJ. "Changes realized from extended bit-depth and metal artifact reduction in CT.", *Med Phys*.;40(6Part1):061711, (2013).
- 14- Huang JY, Eklund D, Childress NL, Howell RM, Mirkovic D, Followill DS, *et al*. "Investigation of various energy deposition kernel refinements for the convolution/superposition method.", *Med Phys*.;40(12):121721, (2013).
- 15- Washio H, Ohira S, Funama Y, Morimoto M, Wada K, Yagi M, *et al*. "Metal artifact reduction using iterative CBCT reconstruction algorithm for head and neck radiation therapy: A phantom and clinical study.", *Eur J Radiol*.;132:109293, (2020).
- 16- Hansen CR, Johansen J, Kristensen CA, Smulders B, Andersen LJ, Samsøe E, *et al*. "Quality assurance of radiation therapy for head and neck cancer patients treated in DAHANCA 10 randomized trial.", *Acta Oncol*.;54(9):1669–73, (2015).
- 17- Bushberg JT, Boone JM. "The essential physics of medical imaging." *Lippincott Williams & Wilkins*; (2011).
- 18- Gardner SJ, Mao W, Liu C, Aref I, Elshaikh M, Lee JK, *et al*. "Improvements in CBCT image quality using a novel iterative reconstruction algorithm: a clinical evaluation.", *Adv Radiat Oncol*.;4(2):390–400, (2019).
- 19- Mao W, Liu C, Gardner SJ, Siddiqui F, Snyder KC, Kumarasiri A, *et al*. "Evaluation and clinical application of a commercially available iterative reconstruction algorithm for CBCT-based IGRT.", *Technol Cancer Res Treat*.;18:1533033818823054, (2019).
- 20- Lee M-J, Kim S, Lee S-A, Song H-T, Huh Y-M, Kim D-H, *et al*. "Overcoming artifacts from metallic orthopedic implants at high-field-strength MR imaging and multi-detector CT." *Radiographics*.;27(3):791–803, (2007).
- 21- Lell MM, Meyer E, Kuefner MA, May MS, Raupach R, Uder M, *et al*. "Normalized metal artifact reduction in head and neck computed tomography.", *Invest Radiol*.;47(7):415–21, (2012).
- 22- Andersson KM, Dahlgren CV, Reizenstein J, Cao Y, Ahnesjö A, Thunberg P. "Evaluation of two commercial CT metal artifact reduction algorithms for use in proton radiotherapy treatment planning in the head and neck area." *Med Phys*.;45(10):4329–44, (2018).